6. Galaxies and star-formation on galactic scales

Equipped with his five senses, man explores the universe around him and calls the adventure Science

— Edwin Hubble

In this chapter, we will review the properties of galaxies in the local Universe, and will discuss the star-formation on galactic scales.

6.1 Properties of Galaxies in the Local Universe

In this section, we will build on the material type you met in relativistic astrophysics and cosmology course.

6.1.1 The Galaxy Zoo

By observing the galaxies in the 1920's, Edwin Hubble identified several morphology: elliptical, spiral, barred spiral and irregular (Figure 6.1). In the following, we will briefly give the properties of each type of galaxies.

Ellipticals - or early type galaxies

The elliptical galaxies are classified following the ratio between their major (a) and minor (b) axis, and named as En, with n defined as :

$$n = 10\frac{a-b}{a} \tag{6.1}$$

They are gas poor galaxies, with no (or little) star formation. Their stellar population is generally dominated by old stars, and their stellar mass is ranging from $10^{11}\mathrm{M}_\odot$ to $10^{13}\mathrm{M}_\odot$. However, dwarf elliptical galaxies have masses of a few $10^{10}\mathrm{M}_\odot$ or less.

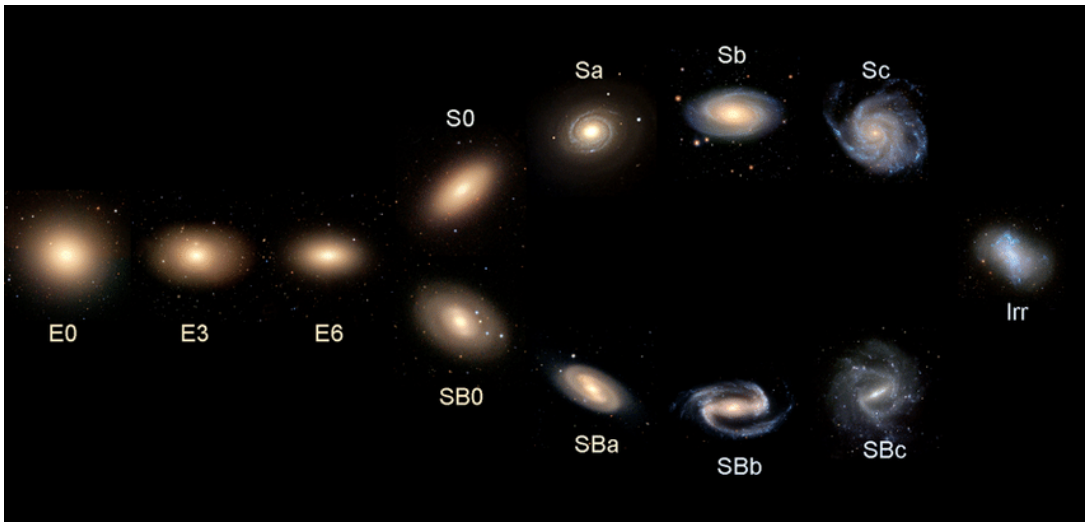

Figure 6.1 : The Hubble sequence with the different types of galaxies : elliptical, spiral, barred spiral and irregular. From Cui et al. (2014)

The surface brightness of an elliptical galaxy is given by :

$$I(R) = I_o \exp\left[-\left(\frac{R}{a}\right)^{1/4}\right] \tag{6.2}$$

Spirals - or late type galaxies

A spiral galaxy is composed of a bright bulge and a disk. They could be either spiral with no bar (named S) or barred spiral (named SB). From Sa to Sc (or SBa to SBc), the openness of arms increases, the prominence of the bulge decreases and the gas content increases. They are more gas rich than ellipticals with at least some star-formation on-going. The gas is both low density neutral hydrogen and dense molecular hydrogen. The fractional mass of neutral hydrogen gas to total (i.e. M(HI)/M) is less than 0.03 for a Sa and goes up to 0.1 for Sc. In the description of a spiral galaxy, we can also include the presence of rings identified with "r" after the name of the spiral (Figure 6.2) and the luminosity of the arms ("I" for well defined arms to "V" to less luminous fuzzy arms ; Figure 6.3).

Firstly we describe the structure of spiral (or barred spiral) galaxy in terms of a near spherical bulge which has similar properties to an elliptical, plus a disc. The simplest description of the system requires a two dimensional model. A spiral seen face-on has a surface brightness profile which follows an exponential distribution

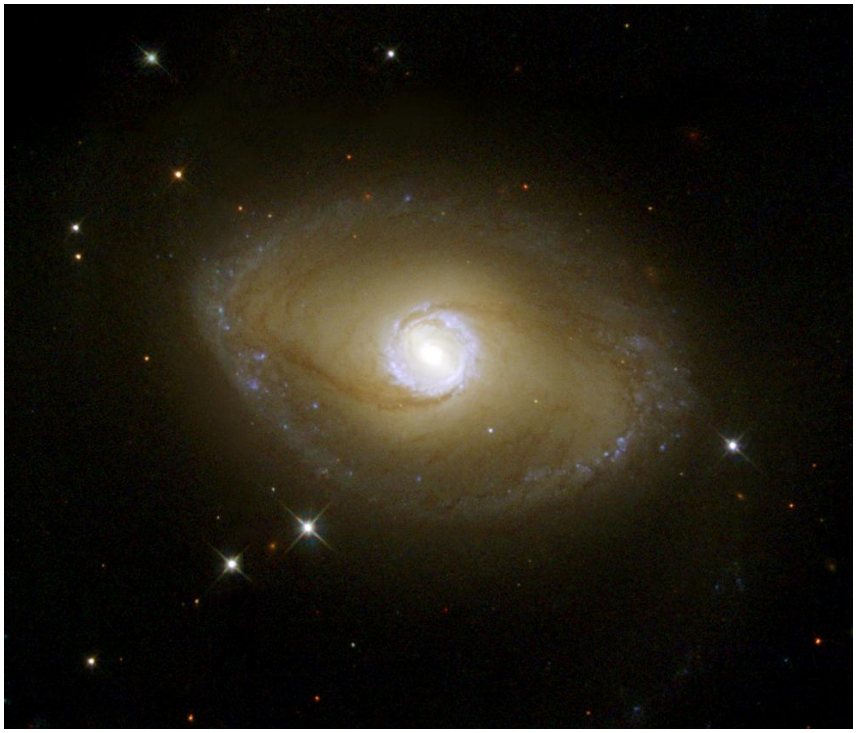

Figure 6.2 : Color image of the galaxy NGC 6782 classified as SB0(r)I. Source : NASA

Figure 6.3 : Color image of the galaxy M83 classified as SBc(s)II. Source : NASA

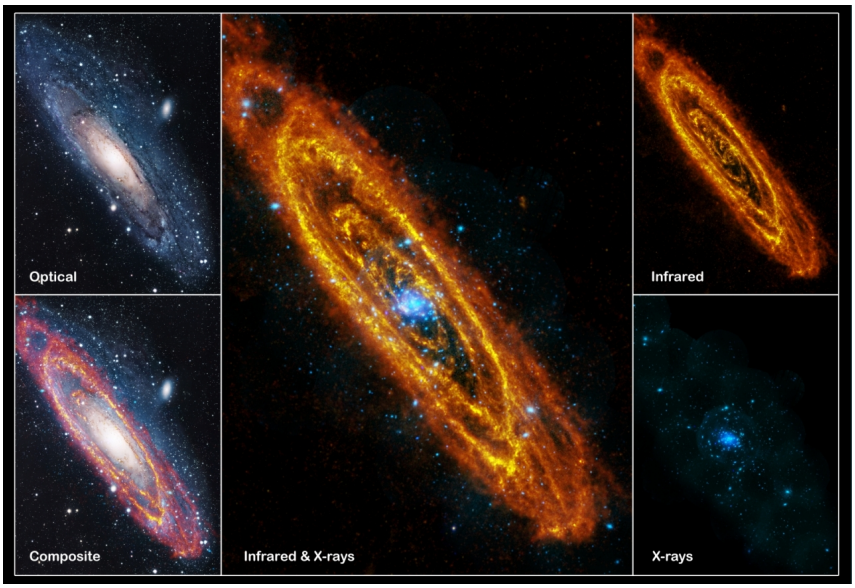

Figure 6.4 : Color image of the galaxy M31 as seen by the Hubble Space Telescope at optical wavelength(top left), by the Herschel telescope in infrared (top right), by the Chandra telescope in X-ray (bottom right). Source : ESA

such as :

$$I(R) = I_o \exp(-\frac{R}{a}) \tag{6.3}$$

The vertical structure in the disk also follows an exponential distribution with a scale height[1] we will call h. This implies an overall mass distribution in the disc of:

$$\rho(R, z) = \rho_0 \exp(-R/a) \exp(-|z|/h) \tag{6.4}$$

The most obvious feature of spiral galaxies, their spiral arms, are a complicated dynamical feature which we will return to later in the course. Here we note that the spiral arms are delineated in many different ways : they are seen in the stellar distribution, atomic and molecular gas, young stars, magnetic fields, etc... (Figure 6.4)

6.1.2 The galaxy Luminosity Function

By definition, the galaxy Luminosity Function is the distribution in luminosity (L) of the number density of galaxies ($\phi(L)$) at a given redshift. Its form has been

[1] bu definition, the scale height is a measure of the decrease of something that falls off exponentially by height, specifically, the height over which it falls by a factor of e (∼2.718)

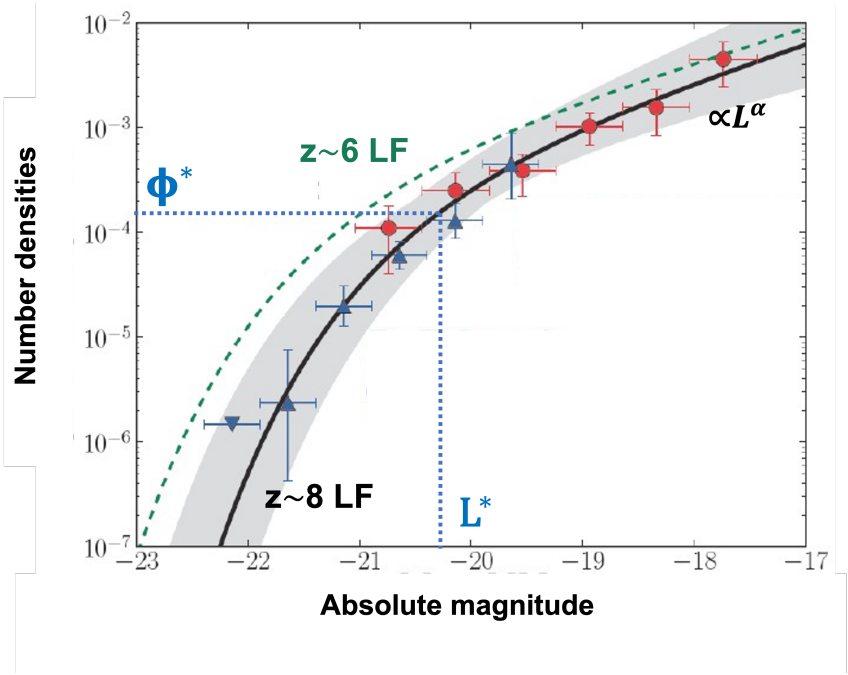

Figure 6.5 : UV Luminosity Function estimated at $z \sim 8$ (black line) compared to the UV Luminosity Function at $z \sim 6$ (green dashed line). The three parameters of the LF are also indicated. Adapted from Schmidt et al. (2014)

described empirically by Schechter (1976) :

$$\Phi(L/L^{\star})d(L/L^{\star}) = \Phi^{\star}(L/L^{\star})^{\alpha}\exp(-(L/L^{\star}))d((L/L^{\star}) \tag{6.5}$$

that we can re-write as :

$$\Phi(x)dx = \Phi^{\star}x^{\alpha}e^{-x}dx \tag{6.6}$$

where $\Phi^{\star}$ and $L_{\star}$ are the density and luminosity where there is a change in the shape of the function (from exponential to linear), and α is the slope at the faint-end of the Luminosity Function.

To determine the number density of galaxies, $\Phi(L)$ we need a redshift survey complete to L_{lim} at a given redshift z. The number of galaxies per given luminosity is not similar to $\Phi(L)$ because of the Malmquist bias which is an effect in observational astronomy which leads to the preferential detection of intrinsically bright objects. In statistics, this bias is referred to as a selection bias or data censoring. It affects the results in a brightness-limited survey, where stars below a certain apparent brightness cannot be included. Since observed stars and galaxies appear

dimmer when farther away, the brightness that is measured will fall off with distance until their brightness falls below the observational threshold. Objects which are more luminous, or intrinsically brighter, can be observed at a greater distance, creating a false trend of increasing intrinsic brightness, and other related quantities, with distance. This effect has led to many spurious claims in the field of astronomy. Properly correcting for these effects has become an area of great focus.

To test the integrity of a survey regardless of the luminosity bias, we can use the volume-luminosity test (also called the V/V_{max} method) develop by Schmidt et al. (1968). The $< V/V_{max} >$ method tests whether the distribution of objects is uniform within the volume of space defined by the observational selection criteria. Among other advantages, it is suitable for samples containing few objects and allows to combine samples of sources obtained with different selection criteria. Historically, it has been employed to study the space distribution of quasars and to assess the cosmic evolution of their population. For a uniform population of sources with measured fluxes S, V/V_{max} are the ratios of the volume V within which each source is distributed to the maximum volume V_{max} within which each source could still be detected (which is individually defined by the sample selection flux limit). In an Euclidean space V/V_{max} should be uniformly distributed between 0 and 1 with an average value $< V/V_{max} >$ =0.5.

Currently the most accurate determination of the UV Luminosity Function of galaxies from $z \sim$4 to 10 has been done by Bouwens et al. (2021) using data from the deepest surveys obtained with the *Hubble* Space Telescope (*Hubble* Ultra Deep Field, CANDELS, Frontier Fields, etc... - Figure 6.6)

6.1.3 Stellar population

Stars are mainly characterised by their luminosity (or mass) and surface temperature. They are classified according to their spectral type (O, B, A, F, G, K, M) which is an ordering in terms of decreasing surface temperature. A diagram showing the luminosity of a star as a function of the temperature is called a *Hertzsprung-Russel* (HR) diagram (Figure 6.7). Most of the stars occupy the region in the diagram along the line called *the main sequence*. During the stage of their lives in which stars are found on the main sequence line, they are fusing hydrogen in their cores. The next concentration of stars is on the horizontal branch (helium fusion in the core and hydrogen burning in a shell surrounding the core). Another prominent feature is the Hertzsprung gap located in the region between A5 and G0 spectral type and between +1 and -3 absolute magnitudes (i.e. between the top of the main sequence and the giants in the horizontal branch). RR Lyrae

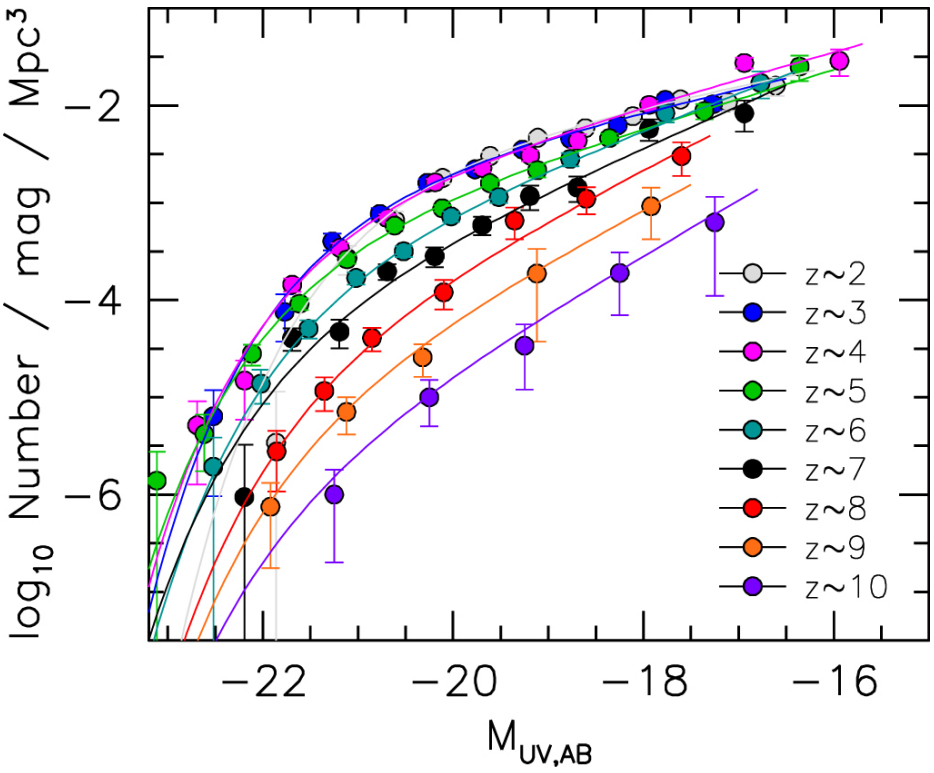

Figure 6.6 : Evolution of the UV Luminosity Function obtained from the analysis of the deepest HST surveys from $z \sim 2$ to $z \sim 10$. A clear decrease in number density if observed from $z \sim 2$ to $z \sim 10$, suggesting a strong decrease in the number of galaxies. We can also see a clear evolution of the characteristic luminosity towards the bright luminosities from $z \sim 10$ to $z \sim 2$ suggesting an increase of the number of bright galaxies with cosmic time. Source : Bouwens et al. (2021)

variable stars can be found in the left of this gap on a section of the diagram called the instability strip. Cepheid variables also fall on the instability strip, at higher luminosities.

The H-R diagram can be used to roughly measure how far away a star cluster or galaxy is from Earth. This can be done by comparing the apparent magnitudes of the stars in the cluster to the absolute magnitudes of stars with known distances (or of model stars). The observed group is then shifted in the vertical direction, until the two main sequences overlap. The difference in magnitude that was bridged in order to match the two groups is called the distance modulus and is a direct measure for the distance (ignoring extinction). This technique is known as main sequence fitting and is a type of spectroscopic parallax.
Stellar luminosity scales approximately as :

$$L \propto M^{\alpha} \tag{6.10}$$

with $\alpha \sim 3$ for stars with mass below $0.5 M_{\odot}$ and $\alpha \sim 4$ for higher masses.
We can also estimate the time a star can remain on the Main Sequence, since the amount of hydrogen is scaled to the stellar mass :

$$\tau_{ms} \propto \frac{M}{L} \propto M^{1-\alpha} \tag{6.11}$$

After this time, stars will evolve off of the main sequence and detailed calculations exist for how this evolution occurs. By applying the previous equation to the most massive stars, it is clear that their lifetime is shorter compared to solar-like stars. Therefore the most massive stars (typically O and B stars) are excellent tracer of recent star-formation. As a consequence of this, UV radiation is generally a good tracer of recent star-formation.

The number of newly formed stars with masses in the range $M \rightarrow M + dM$ is given by the *Initial Mass Function*(IMF), which is commonly taken to have a power-law form (also called Salpeter IMF) :

$$\frac{dN}{dM} \propto M^{\theta} \tag{6.12}$$

where for a standard Salpeter IMF : $\theta = -2.35$
Note that as a consequence of the IMF steeply declining with mass, the bulk of the mass budget is in low mass stars. On the contrary, despite being much less numerous, high mass stars dominate the luminosity, as a consequence of the steep stellar luminosity dependence on the stellar mass.

The Cepheids to probe the distance of nearby galaxies

Cepheids are the first rung in the extragalactic distance ladder and hold a special place in the subject because they were used by Edwin Hubble in his first radial velocity vs. distance plot that led to the discovery of the expanding Universe. Cepheids are a class of variable stars located in the upper H-R diagram (see Figure 6.7); they are evolved, core helium-burning stars whose progenitors are thought to have been B- or late O-type main sequence stars. Their visual magnitudes vary in a regular fashion with amplitudes of between a few tenths of magnitude and ∼2 magnitudes, with periods ranging from a few days to a few weeks. The key role that Cepheids have played in the determination of the extragalactic distance scale stems from the existence of a tight period-luminosity relation: the longer the period of their variability, the brighter their absolute magnitude. Cepheids are supergiant stars with $R \sim 50 R_\odot$ and $L \geq 10^3 L_\odot$, bright enough to be seen over intergalactic distances. Thus by measuring the period of an extragalactic Cepheid star, it is possible to deduce its distance modulus by comparing its observed magnitude with the absolute magnitude, provided the period-luminosity relationship has been calibrated with the known distances of nearby Cepheids in the Milky Way. A later refinement of the calibration includes a colour term, giving the period-luminosity-colour (PLC) relation:

$$M_V = \alpha \log P + \beta (B-V)_0 + \gamma \tag{6.7}$$

where α, β and γ are constants, P the variability period, $(B-V)_0$ the intrinsic $B-V$ colour obtained after correcting for variable extinction Then, including the relation between absolute magnitude and distance :

$$m - M = 5 \log d_{pc} - 5 \tag{6.8}$$

where m is the observed magnitude and d_{pc} is the distance in parsec, therefore

$$d_{pc} = 10^{0.2(\beta[(B-V)_0 + \frac{m}{\beta}] - \alpha \log P + \gamma')} \tag{6.9}$$

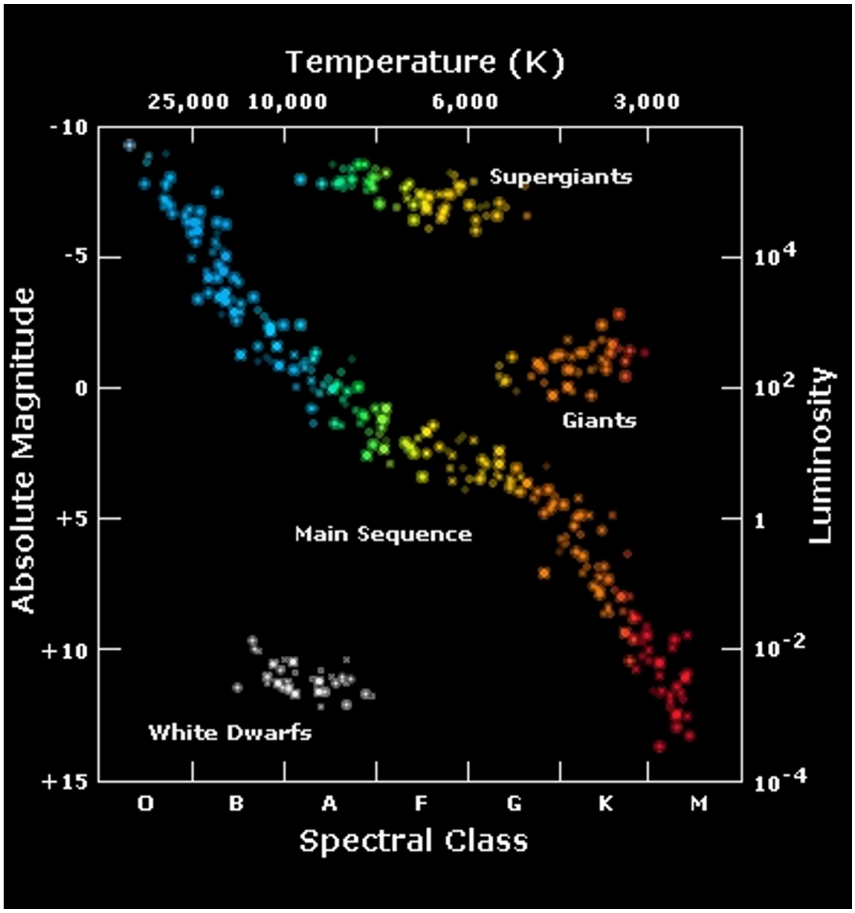

Figure 6.7 : The HR diagram. The position of a star in this diagram gives its nature (giant, dwarfs, etc...). The main sequence is the line on which are most of the stars during their lifetime. Source : NSO

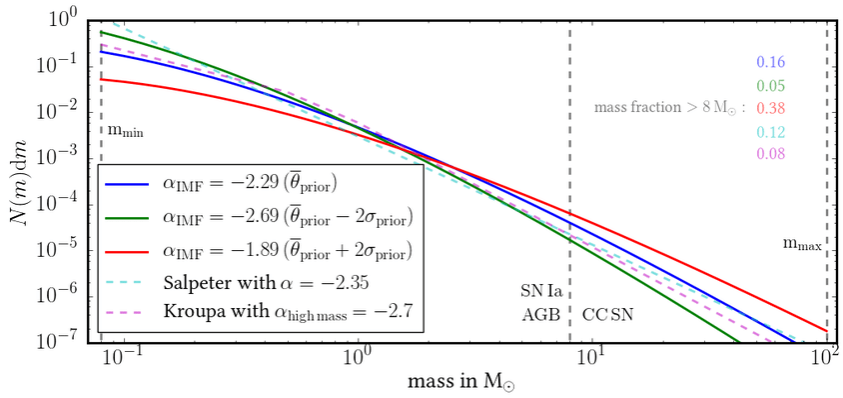

Figure 6.8 : Different Initial Mass function, including the standard Salpeter IMF (in dashed blue line). From Rybizki et al. (2017)

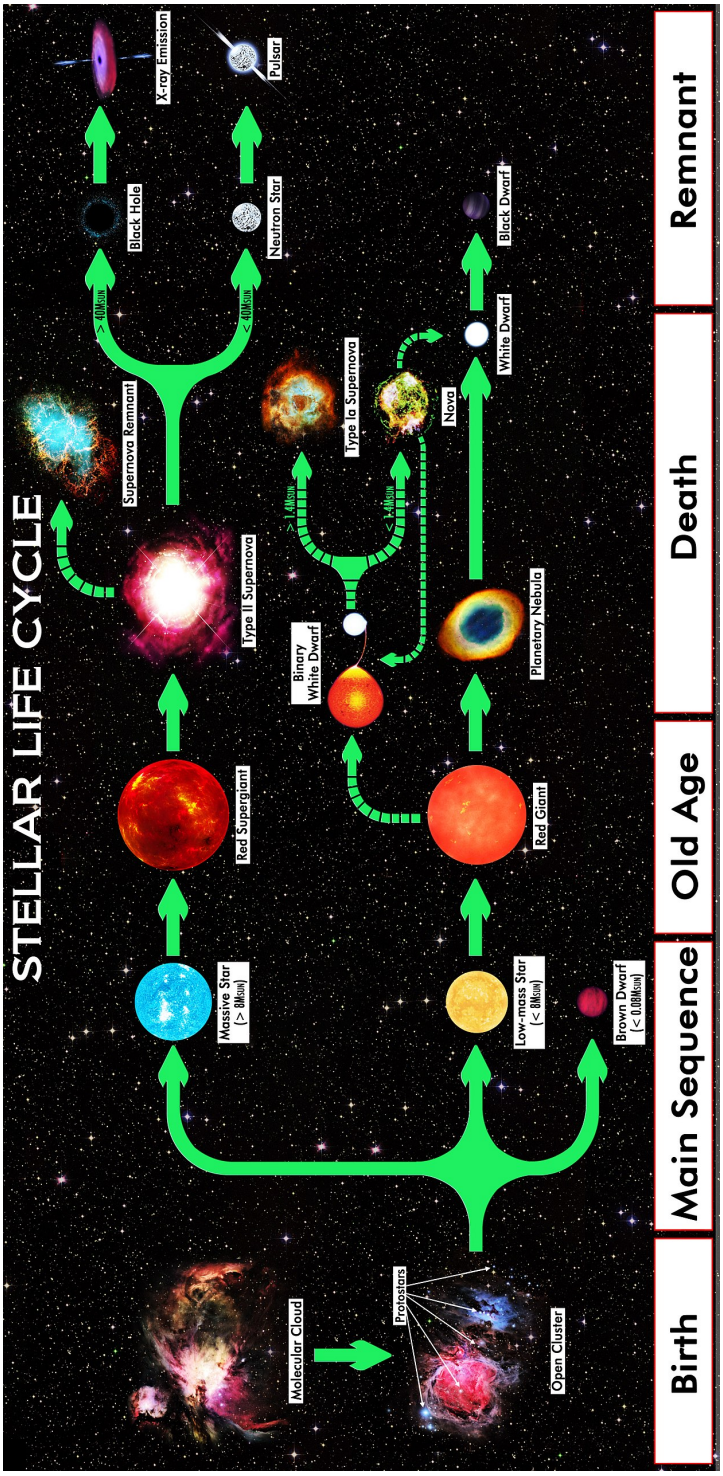

Figure 6.9 : Summary of the life of a star depending on its original mass. Source : R. N. Bailey

6.2 Cloud fragmentation

In the previous chapters, we studied the stability of clouds, but we skipped over an important problem. We saw that the Jeans mass in the ISM was of order the mass of a star. This clearly implies that any more massive cloud also exceeds the Jeans mass and is therefore unstable. Why do we not produce therefore a few very massive collapsed objects (stars ?) from the collapse of a giant molecular cloud ? What we see observationally is that giant molecular clouds are composed of many small dense clouds.

Therefore the scenario that must occurs is the fragmentation of a single massive cloud as it starts to collapse. The current model considers perfectly spherical collapse, anything breaking this symmetry will greatly complicate the physics. To get some insight into how a large cloud might collapse, we return to our analysis of the free-fall timescale.

For a cloud which greatly exceeds its Jeans Mass, it is clear that the gravitational energy is much larger than the thermal energy, and therefore the pressure-free collapse model we used to derive the free-fall time is - at least initially - a reasonable model. Consider again an initially homogeneous spherical cloud of gas of density ρ_0, radius R, and mass M_0 with no internal pressure throughout the collapse. Gas molecules initially at a radius r_0 will have a mass of gas M_r within the radius, and during the collapse this mass remains constant. Therefore the equation of motion for these molecules is :

$$\frac{\partial^2 r}{\partial t^2} = -\frac{GM_r}{r^2} \tag{6.13}$$

Multiplying by $\dot{r} = \frac{dr}{dt}$ and integrating with respect to time gives :

$$\frac{1}{2}\dot{r}^2 = \left[\frac{GM}{r}\right]_{r_0}^{r} = \frac{GM}{r_0}\left(\frac{r_0}{r} - 1\right) = \frac{4\pi}{3} r_0^2 \rho_0 G \left(\frac{r_0}{r} - 1\right) \tag{6.14}$$

hence

$$\frac{dr}{dt} = -\sqrt{\frac{8\pi G \rho r_0^2}{3}} \left(\frac{r_0}{r} - 1\right)^{1/2} \tag{6.15}$$

where the negative sign is chosen to indicate the collapse. This is what we had previously.

Now let's follow this solution by introducing the dimensionless length $\xi = r/r_0$ and the characteristic time $t_0 = \sqrt{3/8\pi G\rho_0}$, and introducing $\tau = t/t_0$. Then :

$$\frac{d\xi}{d\tau} = -\left(\frac{1}{\xi} - 1\right)^{1/2} \tag{6.16}$$

we make the substitution $\xi = cos^2\alpha$, then

$$\frac{d\alpha}{d\tau} = \frac{1}{2cos^2\alpha} \tag{6.17}$$

separating variables and integrating gives :

$$\alpha + \frac{1}{2}sin2\alpha = \tau \tag{6.18}$$

Several conclusions arise from the previous equations :

- The end of collapse occurs when $\xi = 0$, i.e. when $\alpha = \pi/2$ giving :

$$t_{ff} = \frac{\pi}{2}t_0 = \left(\frac{3\pi}{32G\rho_0}\right)^{1/2} \tag{6.19}$$

- The mass within each collapsing shell is conserved, and since the density is initially uniform, it must remain uniform (because t_{ff} does not depend on r_0) and scales such as $r_0^3\rho_0 = r^3\rho(t)$ (constant mass within $r(t)$) or :

$$\frac{\rho(t)}{\rho_0} = \frac{r_0^3}{r^3} = \frac{1}{cos^6\alpha} \tag{6.20}$$

- For a time t close to collapse, we have :

$$\tau = \frac{t}{t_0} = \frac{t_{ff} - (t_{ff} - t)}{t_0} = \frac{\pi}{2} - \epsilon \qquad \text{At this time } r \sim 0 \rightarrow \alpha = \frac{\pi}{2} - \beta \tag{6.21}$$

  Inserting this into eq.6.18 gives, on expanding the "sin" :

$$\beta^3 = \frac{3\epsilon}{2} \tag{6.22}$$

- Then the density close to collapse must be :

$$\frac{\rho(t)}{\rho_0} = \frac{1}{cos^6(\pi/2 - \beta)} = \frac{1}{sin^6\beta} \approx \left(\frac{2}{3\epsilon}\right)^2 = \left(\frac{2t_0}{3(t_{ff} - t)}\right)^2 \tag{6.23}$$

  Note that $\rho(t)/\rho_0$ depends only on t_{ff}, i.e. only on ρ_0, and not on the initial radius r_0.

Now consider that towards the center of the initial sphere the density was perturbed to have a slightly higher density - an overdensity $\rho' = \rho_0 + \delta_0$. This overdensity will have a slightly shorter free-fall time given by :

$$t'_{ff} \approx t_{ff}\left(1 - \frac{\delta_0}{2\rho_0}\right) \tag{6.24}$$

Towards the end of the collapse, this will have grown relative to the mean density of the cloud to :

$$\frac{\rho(t)'}{\rho(t)} \approx \left(\frac{t_{ff} - t}{t'_{ff} - t}\right)^2 \tag{6.25}$$

$$\approx 1 + \frac{\delta_0 t_{ff}}{\rho_0 (t_{ff} - t)} \tag{6.26}$$

Therefore the overdensity grows as :

$$\frac{\delta(t)}{\rho(t)} \approx \frac{\delta_0 t_{ff}}{\rho(t_{ff} - t)} \tag{6.27}$$

This implies that all overdensities (perturbations) grow on the same timescale (i.e. about simultaneous fragmentation). This is different to what we might expect from the Jeans analysis. In the latter, the growth of instabilities of a given mass was exponential and the timescale for growth depended on the wavenumber and hence the mass. Moreover the growth time depended on the wavelength with the largest modes growing fastest.

As a conclusion, we have demonstrated that a small inhomogeneity in the pressure-free case will grow algebraically with time and that all perturbations grow at the same rate. Qualitatively :

- A cloud which is initially very large compared to the Jeans mass will start to undergo approximately pressure-free collapse.
- Many factors will break the symmetry we have considered in our ideal models such as : the initial shape of the cloud, large-scale rotation, small scale velocity variations - turbulence
- Any initial inhomogeneities will grow with time and they all grow on similar timescales
- Eventually we expect the densest of these to become self-gravitating in their own right.

How do we form the Initial Mass Function of stellar masses ?

This is very still uncertain. What we do know observationally is that there is good correspondence between the cloud-mass spectrum and the shape of the IMF. However how does this mass spectrum come about ? Input physics almost certainty includes :

- Turbulence - energy input drives random motions in the gas giving rise to a turbulent cascade. The standard result is that the spectrum of energy in turbulent motion satisfies:

$$E(k)dk \propto k^{-5/3}dk \tag{6.28}$$

- The most successful models invoke scale-free, or fractal, structures within the cloud
- Competitive accretion - for example the denser cores grow by faster than the less dense cores by competing more strongly for the low density gas.

To make further progress requires numerical simulation (Figure 6.10).

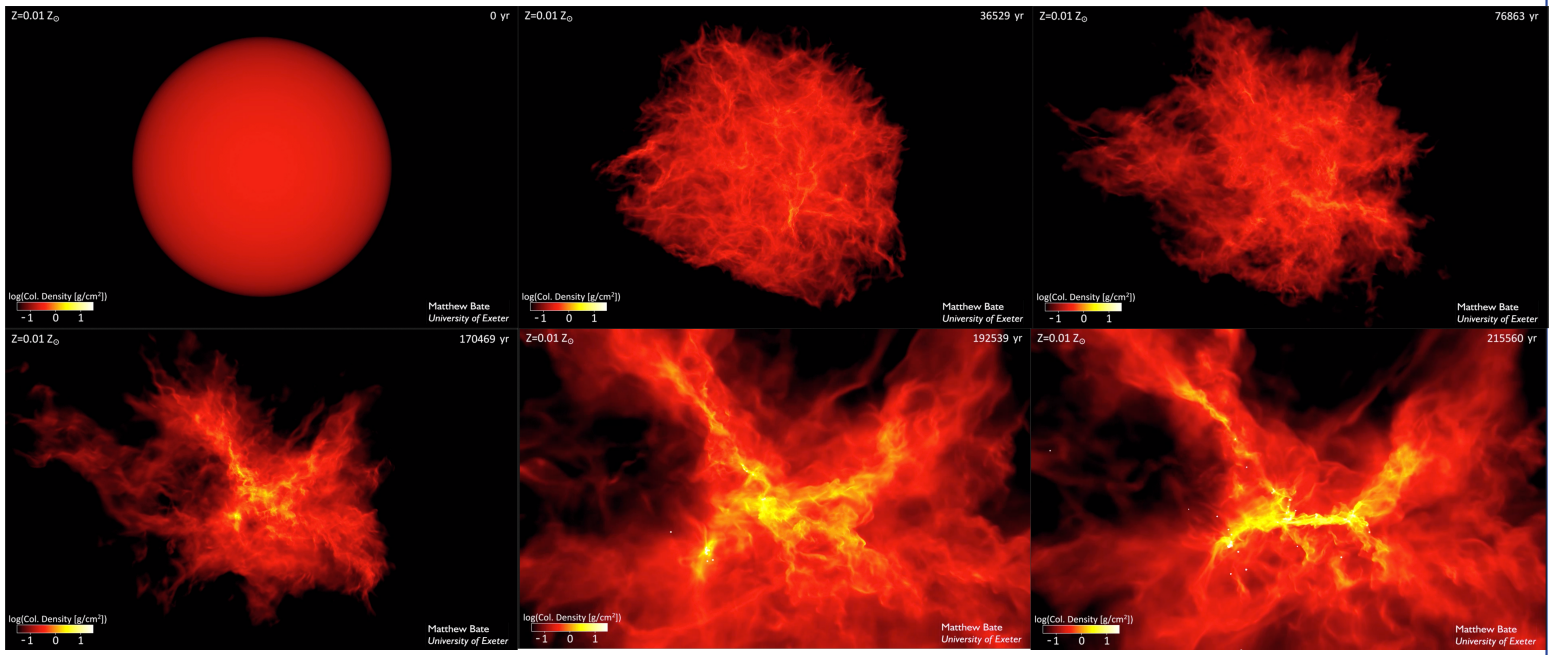

Figure 6.10 : Simulation of the fragmentation of a giant molecular cloud leading to the formation of several stars. Key times are : $t = 0$ initial gas cloud ; t =36kyr clouds of interstellar gas are seen to be very turbulent with supersonic motions ; t =77kyr the turbulent motions in the cloud form shock waves that slowly damp the supersonic motions ; t =170kyr when enough energy has been lost in some regions of the simulation, dense core form ; t =190kyr the formation of stars and brown dwarfs begin in the dense core ; t =210kyr as the stars and brown dwarfs interact with each other, many are ejected from the cloud.

6.3 Galactic-wide star formation

In this section, we consider what factors controls star-formation on a galactic scale. Our main goal is to determine the *star-formation rate* (SFR) for the galaxy (mass of stars formed per unit time). Before going any further, we need to define the following quantities :

- ψ : SFR per unit volume (or possible mass) of the galaxy
- Ψ : SFR for the whole galaxy
- Σ_{SFR} : SFR per unit projected area of a galaxy (a useful observational definition)

We first start by considering observational results. We certainly expect the star formation rate to depend on the amount of available fuel. This is characterised observationally by assuming what is called the *Schmidt law* with :

$$\Sigma_{SFR} \propto \sigma^n \tag{6.29}$$

where σ is the surface gas density. For a constant disc thickness this can be written as :

$$\psi \propto \rho^n \tag{6.30}$$

The best observational results give rise to what we call the *Schmidt-Kennicutt law* (see also Figure 6.11):

$$\frac{\Sigma_{SFR}}{M_\odot yr^{-1}kpc^{-2}} = 2.5 \times 10^{-4} \left(\frac{\sigma}{M_\odot pc^{-2}} \right)^{1.4} \tag{6.31}$$

This result is for the averaged properties of galaxies.

We can now consider some possible simple models for the star formation rate. In all cases, we need to assemble clouds which exceed a Jeans mass and then allow them to collapse.

Collisional assembly

Here we assume that the ISM consists of a large number of small clouds, each less massive than the Jeans mass. Larger clouds are constructed by collisions between the clouds. In this simple case, the collision rate will be of order $n^2 \times v \times A$, where n is the number density of clouds, A their cross section and v the RMS mean (random) velocity in the disc. Also, we assume the collision time is long compared to the free-fall time of the clouds once they exceed their Jeans mass. This suggests that $\psi \propto \rho^2$ which is not in agreement with the Schmidt-Kennicutt law.

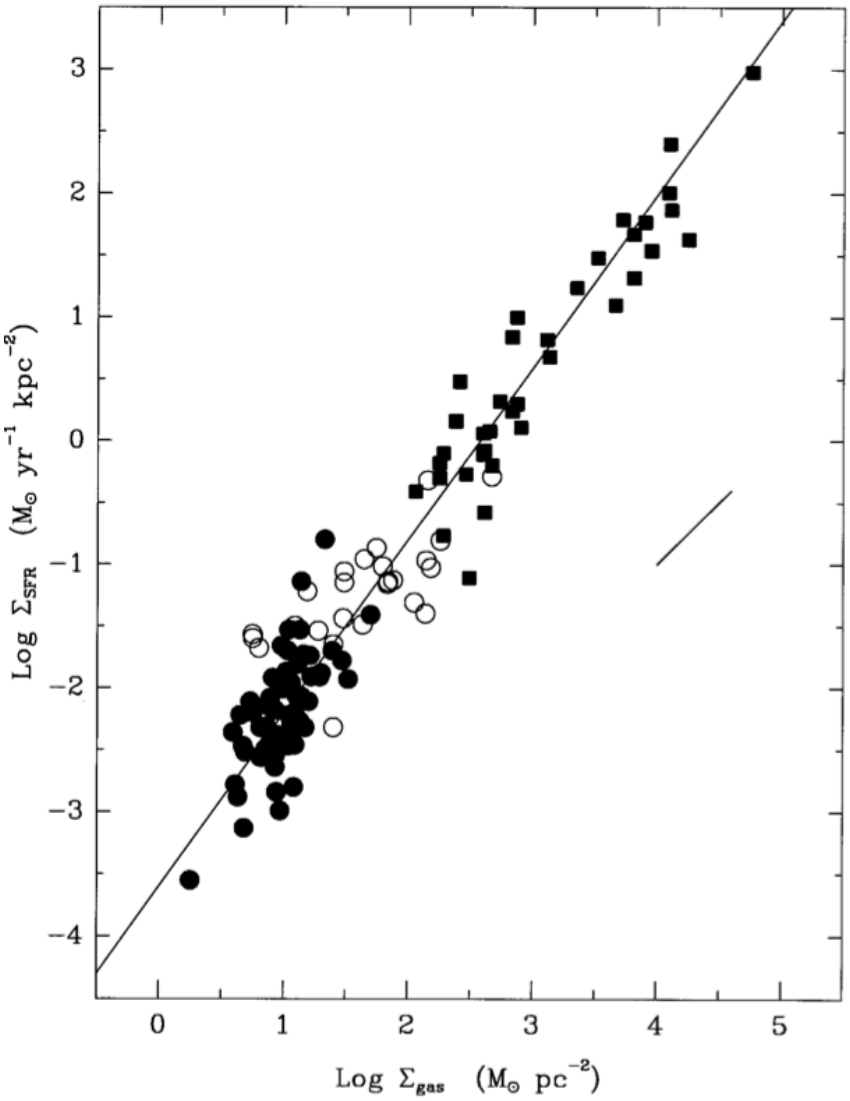

Figure 6.11 : Composite star-formation law for the normal disk (filled circles) and starburst (squares) samples. Open circles show the SFRs and gas densities for the centres of the normal disk galaxies. The line is a least-squares fit with N=1.4. Source : Kennicutt (1998)

Collapse-time limited

An even simpler model is to assume we have large clouds already in place, which exceeds the Jeans mass by a large factor. These will collapse and fragment on a free-fall time as we discussed previously. The SFR will then be determined by the amount of gas which can form stars, which will just be proportional to the density divided by the collapse time scale, such as :

$$\psi \propto \frac{\rho}{t_{ff}} \tag{6.32}$$

but $t_{ff} = (3\pi/32G\rho)^{1/2}$ therefore we get :

$$\psi \propto \rho^{3/2} \tag{6.33}$$

which is close to the Schmidt-Kennicutt law.
However, recent studies have demonstrated that this model is certainly too simplistic and additional effects have to be taken into account.

From the observational point of view, it has been shown that the bulk of the Schmidt-Kennicutt relation is driven by the molecular component of the gas : if the gas surface density is divided into atomic and molecular components, then it becomes observationally clear that the star formation rate (or Σ_{SFR}) does not depend on Σ_{HI} while it depends strongly on Σ_{H2}. This clearly indicates that star-formation is associated with the molecular phase of the gas (where cooling and, therefore, fragmentation, can occur more efficiently). Furthermore, if one considers only the dense component of the molecular gas (i.e. gas with density of about $10^6 \mathrm{cm}^{-3}$ or higher), then the relation with the SFR becomes tighter and linear. Therefore, observations suggest that there is a 1:1 relation between the star formation rate and the mass of the dense component of the molecular gas. The super-linear relation with the total H_2 mass is probably a consequence of the fact that in low density environments, there is an additional diffuse component of the molecular gas that does not participate to the star formation process.

6.4 Simple models of gas and star formation evolution in galaxies

In the following section, we will develop a very simple model of gas in a galaxy to trace the evolution of the star-formation rate. We first need to make the following assumptions :

- The initial total gas mass is M_0

- The mass in the gas is a function of time : $g(t)$
- The mass in stars is given by : $s(t)$
- The star formation rate is given by $\Psi(t)$

Gas is returned from the stars to the ISM via supernovae. We make the approximation that this is an instantaneous process and that the fraction of mass locked up in old stars is α. Gas is therefore returned to the ISM from supernovae at a rate : (1-α)Ψ. This phenomena is called *feedback* and we will discuss it later.

6.4.1 Closed-box model of star formation in a galaxy

For this model, we assume that there is no gas inflow or outflow, i.e. the galaxy evolves as a "closed box". The mass of gas therefore evolves as follows :

$$\frac{dg}{dt} = -\Psi + (1-\alpha)\Psi = -\alpha\Psi \tag{6.34}$$

For simplicity, we can assume a linear relation :

$$\Psi(t) = \epsilon g(t) \tag{6.35}$$

where ϵ can be seen as *the star formation efficiency*, i.e. the mass of stars formed per unit gas mass. We therefore get for the evolution of the mass of gas :

$$\frac{dg}{dt} = -\alpha\epsilon g \tag{6.36}$$

integrating :

$$\ln(g(t)) - \ln(M_0) = -\alpha\epsilon t \tag{6.37}$$

hence :

$$g(t) = M_0 e^{-\alpha\epsilon t} \tag{6.38}$$

Therefore for a galaxy evolving like a closed box, the gas mass decreases exponentially with time.
For the stellar mass :

$$s(t) = M_0 - g(t) = M_0(1 - e^{-\alpha\epsilon t}) \tag{6.39}$$

6.4.2 The effect of inflows and the gas regulator (or "bathtub") model

If we want to develop a more realistic model, we need to assume that galaxies are not evolving as closed boxes : inflows and outflows of gas characterize the life of most galaxies.

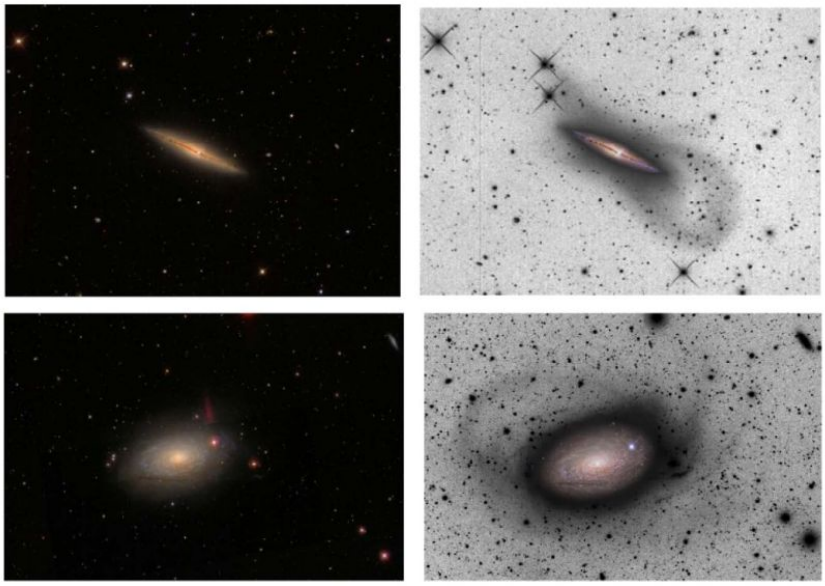

Figure 6.12 : Accreting gas (inflowing gas) in two nearby galaxies. Images on the left from the Sloan Digital Sky Survey of the nearby galaxies NGC 4013 (top) and M63 (bottom) show regular disks while the much deeper images on the right reveal streams of stars accreted from smaller galaxies. From Carlin et al. (2016)

We first focus on gas inflows. The presence of gas inflows was first inferred directly from the analysis of the stellar metallicities in our Galaxy (we will look at this later on). Direct evidence for accreting gas onto the Milky Way was then found through the detection of high velocity gas clouds in the halo of the Milky Way, detected trough HI 21cm observations. Direct evidence for gas accretion has been observed also in other local galaxies (Figure 6.12). According to galaxy evolutionary models, gas inflows are even more prominent and important in high-redshift galaxies.
Suppose now, a galaxy subject to a constant gas inflow rate Φ. Then the evolution of the gas mass becomes :

$$\frac{dg}{dt} = -\alpha\Psi + \Phi \tag{6.40}$$

One may naively expect that a very large inflow rate Φ may produce a galaxy extremely rich in gas, with a total mass completely dominated by the gas mass. However, for the bulk of the galaxies that is not the case. This is because the star formation rate Ψ is linked to the total gas mass through the Schmidt-Kennicutt relation, and it acts as a "valve" that regulates the total amount of gas in the

galaxy, by transforming the excess inflowing gas into stars. More specifically :

$$\frac{dg}{dt} = -\alpha\epsilon g + \Phi \tag{6.41}$$

As the inflow deposit gas onto the galaxy, the gas mass g increases until the point where the right hand term of eq.6.41 becomes 0. At this point the gas content of the galaxy is in equilibrium, i.e. any inflowing gas is transformed into stars. Therefore equilibrium occurs when the gas mass in the galaxy is :

$$g = \frac{\Phi}{\alpha\epsilon} \tag{6.42}$$

This scenario is often dubbed "bathtub" model, where the gas inflow can be seen as water flowing from the tab, the gas mass can be seen as the water in the bathtub, while the star formation rate is the water flowing out of the drain. The rate at which water flows out of the drain is proportional to the water pressure, hence proportional to the amount of water in the bathtub. The amount of water in the bathtub reaches a level where its pressure onto the drain makes the rate of outflowing water equal to the rate of inflowing water. If the rate of inflowing water from the tap is increased or decreased, the level of water in the bathtub increases or decreases to reach a new equilibrium point, where the associated pressure makes the outflow rate again in equilibrium with the inflow rate. Conceptually, the amount of gas in a galaxy works in a similar way, where the water pressure is replaced by the Schmidt-Kennicutt law.

It is often useful to define the *gas fraction*, which is the mass of the gas relative to the total baryonic content (i.e. gas and stars), which is often an indicator of evolutionary stage of a systems :

$$f_{gas} = \frac{M(gas)}{M(baryons)} = \frac{M(gas)}{M(gas) + M(star)} = \frac{g}{g+s} \tag{6.43}$$

We have seen that for a constant inflow rate, at equilibrium, the gas mass is constant, and given by eq.6.42. However, the stellar mass keeps growing and it is given by :

$$s = \Phi t - g \tag{6.44}$$

N.B.: This is true only when the galaxy has reached equilibrium.
Therefore, the gas fraction steadily decreases with time, hence making galaxies "gas poor" as :

$$f_{gas} = \frac{1}{\alpha\epsilon t} \tag{6.45}$$

Once more, this is correct only after the equilibrium has been reached and neglecting the stellar mass produced before reaching equilibrium, i.e. when $t >> 1/\alpha\epsilon$. This implies that the gas fraction is independent of the inflow rate.

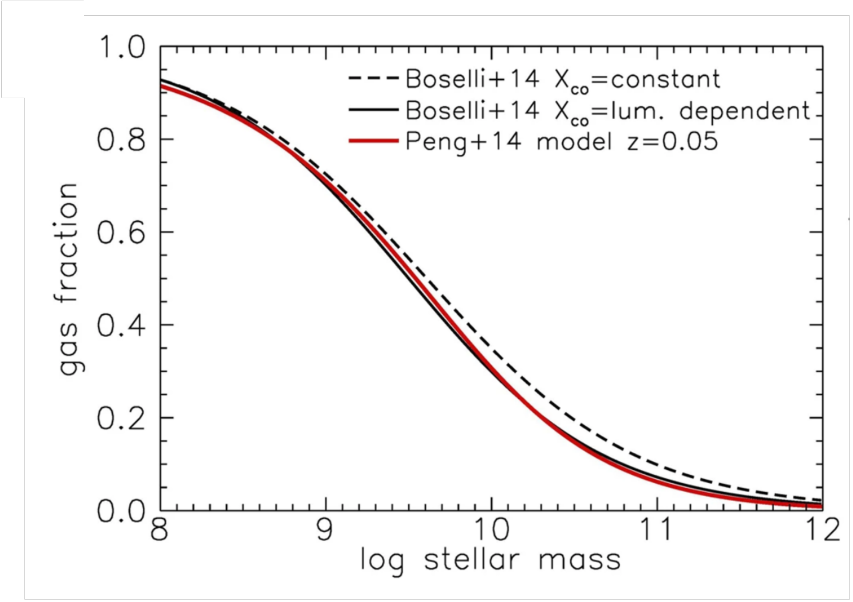

Figure 6.13 : Evolution of the gas fraction as a function of the stellar mass observed in local galaxies. From Peng et al. (2015)

Note that the gas fraction is also indirectly related to the stellar mass. Indeed also the stellar mass depends on time, according to equation 6.44. The gas fraction can also be expressed as :

$$f_{gas}(t) = \frac{\Phi + 1}{\alpha \epsilon s(t)} \tag{6.46}$$

which highlights the (indirect) relation between stellar mass and gas fraction. In particular, it is expected that the gas fraction should decrease with stellar mass, which is indeed observed in local galaxies, as shown in Figure 6.13
Note that these equations are also highlighting that the gas fraction is a good tracer of the galaxy evolutionary stage, i.e. galaxies with low gas fraction are typically more evolved than galaxies with high gas fraction.

6.4.3 The effect of outflows

There is a clear observational evidence that prominent outflows eject large mass of gas out of galaxies. This will be seen in more detail in the next lectures, especially when introducing the concept of "feedback". Here we only mention that one of the primary mechanisms responsible for driving outflows is associated to supernova explosions. Radiation pressure (on dust) from the light emitted by young, luminous stars is another possible mechanism. Since both the supernova rate and radiation

from young stars are proportional to the star formation rate, the outflow rate Λ is often conveniently expressed as proportional to the star formation rate :

$$\Lambda = \lambda\Psi \tag{6.47}$$

where λ is often called the "outflow loading factor" (observational constraints generally give $\lambda \sim 1$ for actively star forming galaxies).
By introducing the effect of outflows, the variation of gas with time becomes :

$$\frac{dg}{dt} = -\alpha\Psi + \Phi - \lambda\Psi \tag{6.48}$$

or, by replacing the linear Schmidt-Kennicutt relation :

$$\frac{dg}{dt} = -\alpha\epsilon g + \Phi - \lambda\epsilon g \tag{6.49}$$

which gives an equilibrium gas mass (right hand term to zero) :

$$g = \frac{\Phi}{(\alpha + \lambda)\epsilon} \tag{6.50}$$

So the effect of outflows is similar to that of varying the value of the constant α. The stellar mass at equilibrium (neglecting the stellar mass formed before reaching equilibrium) is given by $s \approx \alpha\Psi t = \alpha\epsilon g t$. Therefore, at equilibrium, the gas fraction is still given by :

$$f_{gas} \approx \frac{1}{\alpha\epsilon t + 1} \approx \frac{1}{\alpha\epsilon t} \tag{6.51}$$

The gas outflows seems not to have an effect in explaining the lower gas fraction in massive galaxies. However, as we shall see later on, in massive galaxies Active Galactic Nuclei (i.e. supermassive accreting black holes) can greatly contribute to enhance the outflow rate, hence effectively increasing the value of λ, even by a factor of several, in massive galaxies, hence contributing to greatly reduce the gas content in massive galaxies.

6.5 Metallicity evolution of galaxies

With the term "metals" astronomers refer to all elements heavier than helium. The mass fraction of heavy elements, also called the metallicity, is indicated with Z and defined by :

$$Z = \frac{M_{metals}}{M_{tot}} \approx \frac{M_{metals}}{M_H} \tag{6.52}$$

It is generally important to differentiate between stellar metallicity (mass fraction of metals in the stellar atmospheres) and gas metallicity (mass fraction of metals in the interstellar medium). The solar metallicity is $Z_{\odot}$=0.014
Except for some lithium and beryllium, metals are produced by stellar (and explosive) nucleosynthesis and released into the Inter Stellar Medium (ISM) at the end of the stellar lifetime trough supernova explosion and stellar winds. The metals injected into the ISM are then used by the formation of the next generation of stars. Different supernovae (hence stars with different masses) enrich the ISM with different elements. Stars with mass larger than $8M_{\odot}$ leave the Main Sequence in less than about 30 Myr and finish their life as type II (core-collapse) supernovae, which enrich the ISM mostly with α-elements[2] (O, Ne, Mg, Si, S, Ca, ...). Stars with mass less than $8M_{\odot}$ take much longer to leave the Main Sequence (e.g. 1 Gyr or longer, depending on their mass). These stars evolve as Asymptotic Giant Branch stars (AGBs) and then Planetary Nebulae, which enrich the ISM mostly with carbon and nitrogen, and then can yield type Ia Supernovae, which inject into the ISM mostly Fe-peak elements.

Modelling the metallicity evolution of galaxies is a very complex field of astrophysics. Multiple effects have to be taken into account (e.g. production of different elements on different timescales, effects of gas inflows diluting the gas metallicity, effect of gas outflows ejecting metals out of the galaxy, variation of the star formation efficiency). The reward is that the comparison between the metallicity predicted by models and observations can provide tight constraints on the galaxy evolutionary scenarios.

It is beyond the scope of this course to investigate in detail the galaxy metallicity evolutionary models and scenarios. In the following, we will only focus on the metallicity evolution in the case of a closed box system that, although relatively simple, provide some interesting information on galaxy evolution.

Metallicity evolution in a closed box system

We recall the basic definitions and assumptions that we introduced for the closed box model :

- The system is closed with no mass loss or gain :
  - Total mass M_0
  - Mass in gas : $g(t)$

[2]The α process, also known as the α ladder, is one of two classes of nuclear fusion reactions by which stars convert helium into heavier elements, the other being the triple-alpha process. The

  - Mass in stars : $s(t)$
  - Star Formation Rate : $\Psi(t)$

- Gas is returned from stars to the ISM via supernovae at a rate (1-α)Ψ
- We also follow the metallicity of the gas, i.e. the mass fraction of heavy elements in the gas :
  - The production of new metals per mass of stars is p
  - The rate of mass of new metals returned to the ISM via supernovae is therefore $p(1-\alpha)\Psi$
  - The total mass of metals returned to the ISM via supernovae is $(p + Z)(1-\alpha)\Psi$

We recall that the mass of gas in a closed box system evolves as follows :

$$\frac{dg}{dt} = -\Psi + (1-\alpha)\Psi = -\alpha\Psi \tag{6.53}$$

The production of metals is given by :

$$\frac{d(gZ)}{dt} = (p+Z)(1-\alpha)\Psi - Z\Psi = p(1-\alpha)\Psi - \alpha Z\Psi \tag{6.54}$$

Combining these two equations gives :

$$g\frac{dZ}{dt} = p(1-\alpha)\Psi = -p\frac{1-\alpha}{\alpha}\frac{dg}{dt} = -P\frac{dg}{dt} \tag{6.55}$$

where P is called the "yield" in this context. Note that this is a differential equation relating the metallicity and gas mass and in this simple case does not depend on the star formation rate which could have any form ; the previous equation can therefore be rewritten as :

$$dZ = -P\frac{dg}{g} \tag{6.56}$$

We can easily integrate this equation using the boundary conditions $t = 0$, $Z = 0$; $g = M_0$ and for a general time t we get :

$$Z(t) = -P\ln(g/M_0) \tag{6.57}$$

$$g(t) = M_0\exp(-Z/P) \qquad \text{and} \qquad s(t) = M_0 - g(t) = M_0(1-\exp(-Z/P)) \tag{6.58}$$

Models of stellar evolution suggest a value for the yield of about $0.5Z_\odot$ where $Z_\odot$ is the solar metallicity.

Stars formed at a time $t < t_1$ must have a metallicity less than $Z(t_1)$ since they formed out of gas which was less enriched in the past (keep in mind that the metallicity observed on the photospheres of Main Sequence stars reflect the metallicity of the gas out of which these were formed since during the Main Sequence there is no mixing between the stellar interior, where nucleosynthesis occurs, and the photosphere). Therefore, for example, the fraction of stars with metallicities less than 0.1 of the solar value ($Z_\odot$) is given by :

$$\frac{s(< Z_\odot/10)}{M_0} = 1 - \exp(-Z_\odot/10P) \approx 1 - \exp(-1/5) \approx 0.2 \qquad (6.59)$$

The problem is that this is much larger than the number of old low-metallicity stars observed in the disc of our galaxy. This problem is commonly called *G-dwarfs problem*. Our star is itself an old G-star with a relatively high metallicity.

There are of course many ways to improve the above model and solve this problem. The most likely solution (broadly accepted), which also hints at our cosmological models for galaxy evolution, as already discussed, is to allow for inflow and outflow of gas. Gas inflows in particular are thought to be the key ingredient to explain the G-dwarfs problem. Even if the inflowing gas has very low metallicity, the G-dwarf problem can be solved because the additional gas can prolong the duration of star formation (relative to the closed box system), hence there are more stars formed at late times, when the gas has already been enriched with metals.

6.6 Stellar orbits and spiral structure

In the previous sections, we have seen that star-formation should occur in regions of overdensities, i.e where it is more likely that gas clouds are compressed, perturbed and collapse to form stars. Observationally we see that this happens in the spiral arms of disk galaxies or at the edges of stellar bars. In the following we investigate the dynamics behind the formation of spiral arms and bars, and the physical conditions that lead to disk instabilities. We will first start by recalling the basic properties of the rotation curves in spiral galaxies.

6.6.1 Rotation curves in galaxy disks

By using spectral lines, such as the neutral hydrogen (HI) at 21cm, or optical nebular emission lines (e.g. Hα), we can measure the rotation curve (the rotation velocity as a function of radius) with accuracy. Disk rotation curves are characterized by a central region (a few kpc in radius at most) where the rotation velocity

triple-alpha process consumes only helium, and produces carbon.

Figure 6.14 : Color image of a spiral galaxy (M101). The star formation is traced by the blue light, and occurs mainly in the arms. Source : STFC

scales linearly with radius ($v(r) \propto r$, i.e. the angular velocity $\Omega_r \sim$ constant). We can therefore estimate the mass within a radius r by applying Gauss's theorem, assuming a spherical mass distribution and circular orbits :

$$\frac{v^2}{r} = \frac{GM(r)}{r^2} \tag{6.60}$$

For a velocity independent of radius, this implies $M(r) \propto r$ which is clearly not consistent with the density distribution of stars, which is inferred from the observed stellar surface brightness, neither with the mass in gas. The conclusion is that there must be more mass - dark matter - than suggested by the distribution of visible matter (stars and baryonic gas). We note that $M(r) \propto 1/r^2$, which is what we expect in a simple model for a dark matter halo.

6.6.2 Stellar Orbits

To simplify the study, we consider a cylindrically symmetric model in which the potential is given by $\Phi(r, z)$ and examine orbits initially in the z =0 plane. We assume the following :

- The angular momentum per unit mass for each star is conserved :

$$l = r^2\phi = \text{constant} \tag{6.61}$$

  where ϕ is the azimuthal angle

- The energy per unit mass is also conserved, therefore :

$$E = \frac{1}{2}\dot{r}^2 + \frac{1}{2}(r\dot{\phi})^2 + \Phi(r) = \frac{1}{2}\dot{r}^2 + \frac{l}{2r^2} + \Phi(r) \tag{6.62}$$

- The equation of motion in the radial direction is just :

$$\ddot{r} - r\dot{\phi}^2 = -\frac{\partial\Phi}{\partial r} \tag{6.63}$$

- It is useful to introduce the effective potential :

$$\Phi_e = \Phi + \frac{l^2}{2r^2} \tag{6.64}$$

  to rewrite the equation of motion :

$$\ddot{r} = -\frac{\partial\Phi_e}{\partial r} \tag{6.65}$$

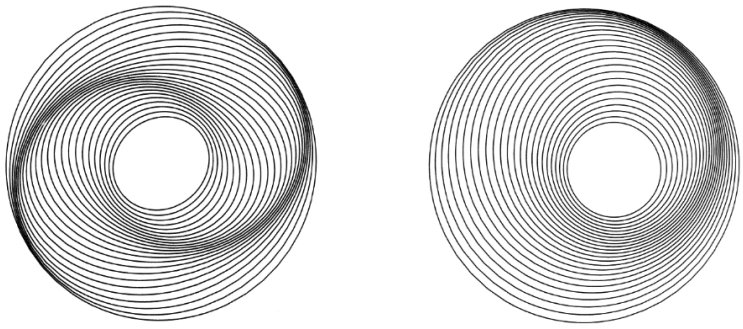

Figure 6.15 : Resonant spiral perturbation

By definition, circular orbits have $\ddot{r} = 0$ and hence are given by :

$$\frac{\partial \Phi_e}{\partial_r}\Big)_{r_0}) = 0 = \frac{\partial \Phi}{\partial r}\Big)_{r_0} - \frac{l^2}{r_0^3} \tag{6.66}$$

where r_0 is the radius of the circular orbit.

Given a $\Phi(r)$, or equivalently a mass distribution, we can calculate the properties of the circular stellar orbit at any radius. In particular at a radius r the angular velocity of the circular orbit is given by :

$$\Omega(r)^2 = \frac{l^2}{r^4} = \frac{1}{r}\frac{\partial \Phi}{\partial r} \tag{6.67}$$

A star when perturbed will undergo small motions about this circular orbit. We write $x = r - r_0$ and expand the effective potential about r_0 :

$$\Phi_e(x) = \Phi_e(r_0) + x\frac{\partial \Phi_e}{\partial r}\Big)_{r_0} + \frac{1}{2}x^2\frac{\partial^2 \Phi_e}{\partial r^2}\Big)_{r_0} + O(x^3) \tag{6.68}$$

The term in x clearly is zero and the radial equation is just :

$$\ddot{x} = -\frac{\partial \Phi_e}{\partial x} = -x\frac{\partial^2 \Phi_e}{\partial r^2}\Big)_{r_0} \tag{6.69}$$

which is the Simple Harmonic Motion (SHM) with a frequency called the *epicyclic*

frequency given by :

$$\kappa^2 = \frac{\partial^2 \Phi_e}{\partial r^2}\Big)_{r_0} = \left[\frac{\partial^2 \Phi}{\partial r^2} + \frac{3l^2}{r^4}\right]_{r_0} \tag{6.70}$$

$$= \left[r\frac{\partial \Omega^2}{dr} + 4\Omega^2\right]_{r_0} \tag{6.71}$$

$$= 4\Omega^2\left[1 + \frac{r}{2\Omega}\frac{\partial \Omega}{\partial r}\right]_{r_0} \tag{6.72}$$

Similarly, we can show that for small amplitude motion out of the plane of the disc (z direction) the star undergoes SHM with :

$$v^2 = \left.\frac{\partial^2 \Phi_e}{\partial z^2}\right|_{r=r_0, z=0} \tag{6.73}$$

6.6.3 Resonant orbits

In general spiral structure is complicated, but one important physical idea is the concept of resonant orbits. Near circular orbits will be the superposition of the pure circular orbit plus the radial motion. In the lab frame after one radial oscillation of period $T_r = 2\pi/\kappa$ the orbit will have precessed by :

$$\Delta\phi \approx \Omega T_r \tag{6.74}$$

In general the orbit will not close in this frame, but consider the situation in a frame rotating at Ω_p - the *pattern speed*. In this frame :

$$\Delta\phi_p = \Delta\phi - \Omega_p T_r \tag{6.75}$$

For the orbit to close after m radial oscillations, we require :

$$2n\pi = \Omega m T_r - \Omega_p m T_r \tag{6.76}$$

or

$$\Omega_p = \Omega - \frac{n}{m}\kappa \tag{6.77}$$

Interestingly, in many systems the form of $\Omega(r)$ means that, for $n = 1$ and $m = 2$, Ω_p is approximately constant across the disk of the galaxy.

In this case, we can arrange the phase of the orbits so that adjacent stars in certain regions of the disk have a higher density and put them on the $n = 1$, $m = 2$, perturbed orbits - these will then be long lived. We can achieved this, for example, if there is an external perturbation, which causes a rotating potential which is resonant with these orbits. There is a lot more to spiral structure than this simple analysis, but the idea of resonant orbit plays a central role.

6.6.4 Stability of a rotating disc - spiral density waves

We now consider the stability of a rotating disc in more detail. One manifestation of unstable discs are spiral density waves, but the following analysis will also provide an insight into the overall stability of the disc and star formation.
We start again with Euler's equations for an ideal fluid. We use a cylindrical coordinate system. The radial equation is :

$$\rho\frac{\partial v_r}{\partial t} + \underbrace{\rho v_r\frac{\partial v_r}{\partial r} + \rho\frac{v_\theta}{r}\frac{\partial v_r}{\partial \theta} - \frac{\rho}{r}v_\theta^2}_{[\rho(v\cdot\nabla)v]_r} = \rho\frac{\partial \phi_g}{\partial r} - \frac{\partial p}{\partial r} \tag{6.78}$$

where ϕ_g is the gravitational potential. The θ equation is :

$$\rho\frac{\partial v_\theta}{\partial t} + \underbrace{\rho v_r\frac{\partial v_\theta}{\partial r} + \rho\frac{v_\theta}{r}\frac{\partial v_\theta}{\partial \theta} - \frac{\rho}{r}v_\theta v_r}_{[\rho(v\cdot\nabla)v]_\theta} = -\rho\frac{1}{r}\frac{\partial \phi_g}{\partial \theta} - \frac{1}{r}\frac{\partial p}{\partial \theta} \tag{6.79}$$

and the equation of continuity :

$$\frac{\partial \rho}{\partial t} + \frac{1}{r}\frac{\partial}{\partial r}(\rho r v_r) + \frac{1}{r}\frac{\partial}{\partial \theta}(\rho v_\theta) = 0 \tag{6.80}$$

We are not interested here in the vertical structure in the disc and therefore we project these equations into a 2D form by integrating the pressure in the z-direction and assuming all of the mass is concentrated in a plane.
If we assume there is no dependence of the velocities on z then this integration gives identical equations except that the density and pressure are replaced by:

$$\rho(r,\theta,z,t) = \sigma(r,\theta,z)\delta(z) \qquad ; \qquad P = \int \rho\,\mathrm{d}z \tag{6.81}$$

where σ is the disk surface density. To proceed, we will use a perturbation analysis. The unperturbed solution is an axially symmetric rotating mass distribution, $\sigma_0(r)$, with v_0=$(0, r\Omega(r))$ and an unperturbed potential ϕ_{g_0}. To these we add on small perturbations, which are all functions of r, θ, and t :

$$v = (u, v + r\Omega) \tag{6.82}$$
$$\sigma = \sigma_0(r) + \sigma'(r,\theta,t) \tag{6.83}$$
$$\phi_g = \phi_{g_0} + \phi'_g(r,\theta,z,t) \tag{6.84}$$

where $\sigma_0(r)$ and $\sigma'(r,\theta,t)$ satisfy :

$$\nabla^2\phi_{g_0} = 4\pi G\sigma_0\delta(z) \qquad \nabla^2\phi'_g = 4\pi G\sigma'(r,\theta,t)\delta(z) \tag{6.85}$$

P is a force per unit length and is of course the plane (2D) analogue of pressure. We assume an isothermal-like equation of state and write :

$$P = a_0^2 \sigma \tag{6.86}$$

where a_0 is essentially the velocity dispersion of the particles – stars – in the disk. Keeping only terms to first order in small quantities, we obtain after some algebra:

$$\text{Radial } u \qquad \frac{\partial u}{\partial t} + \Omega \frac{\partial u}{\partial \theta} - 2v\Omega = -\frac{a_0^2}{\sigma_0}\frac{\partial \sigma'}{\partial r} - \frac{\partial \phi_g'}{\partial r} \tag{6.87}$$

$$\text{Angular } v \qquad \frac{\partial v}{\partial t} + \Omega \frac{\partial v}{\partial \theta} + \frac{\kappa^2 u}{2\Omega} = -\frac{a_0^2}{r\sigma_0}\frac{\partial \sigma'}{\partial \theta} - \frac{1}{r}\frac{\partial \phi_g'}{\partial \theta} \tag{6.88}$$

$$\text{Continuity} \qquad \frac{\partial \sigma'}{\partial t} + \frac{1}{r}\frac{\partial}{\partial r}(r\sigma_0 u) + \frac{\sigma_0}{r}\frac{\partial v}{\partial \theta} + \Omega \frac{\partial \sigma'}{\partial \theta} = 0 \tag{6.89}$$

κ is the epicyclic frequency we introduced earlier and comes into the equations since:

$$u\frac{\partial r\Omega}{\partial r} + u\Omega = 2\Omega u\left(1 + \frac{r}{2\Omega}\frac{\partial \Omega}{\partial r}\right) = \frac{u\kappa^2}{2\Omega} \tag{6.90}$$

We now look for spiral-like solutions writing :

$$\sigma' = \hat{\sigma}\exp\left[i(\omega t - n\theta + \Psi(r))\right] \tag{6.91}$$

with similar expressions for u, v and ϕ_g'. We make the further approximations that $\hat{\sigma}$ are approximately constant functions. The basic properties of solutions of this form are :

- The maximum in the density occurs for $\omega t - n\theta + \Psi(r) = 0$. To understand the implications of this form consider $t = 0$, then the locus of the maximum density has : $n\theta{=}\Psi(r)$ which is a spiral patter which represents n-armed spiral ; and the pattern makes an angle to the θ direction, the pitch angle, $\tan\alpha = \frac{n}{r\frac{d\Psi}{dr}} = \frac{n}{kr}$ where we define k as $k = \frac{d\Psi}{dr}$

- The radial distance between maxima is given by :

$$\Psi(r+\lambda) - \Psi(r) = 2\pi n \tag{6.92}$$

$$\text{For } \lambda << r : \Psi(r+\lambda) \approx \Psi(r) + k\lambda \text{ and } \lambda \approx 2\pi n/|k| \tag{6.93}$$

- The spiral pattern represent advances in time as the *pattern speed* :

$$\Omega_p = \dot{\theta} = \omega/n \tag{6.94}$$

Substituting these spiral-like solutions into eq.6.80 and eq.6.81 leads to a straightforward algebraic equations. Solving Poisson's equation is more difficult. The solution can be found in what is called the tight-winding approximation when $n/kr << 1$ - this implies, among other things, that the main variation in the gravitational potential is radial and not in the angular direction.
We will quote the results of this analysis :

$$\kappa^2 - n^2(\Omega_p - \Omega)^2 + k^2 a_0^2 = 2\pi G|k|\sigma_0 \tag{6.95}$$

or re-arranging :

$$n^2(\Omega_p - \Omega)^2 = (\omega - n\Omega)^2 = \kappa^2 + k^2 a_0^2 - 2\pi G|k|\sigma_0 \tag{6.96}$$

A special case is when the disc is not rotating. We can find the dispersion relation for this special case by setting $n\Omega = 0$ and $\kappa = 0$ to give:

$$\omega^2 = k^2 a_0^2 - 2\pi G|k|\sigma_0 \tag{6.97}$$

This is the dispersion relation we discussed before identifying a_0 as the isothermal sound speed a_T. Returning to the rotating disc, the limiting situation occurs when n is zero (i.e. axisymmetric disc), then:

$$\omega^2 = \kappa^2 + k^2 a_0^2 - 2\pi G|k|\sigma_0 \tag{6.98}$$

the disc is stable to the spiral perturbations provided that $\omega^2 > 0$. From the previous equation it is clear that the rotation (κ) and velocity dispersion (a_0) have both a stabilising effect, while gravity (i.e. the surface density σ_0) has a destabilising effect:

$$\frac{\omega^2}{\kappa^2} = 1 + \frac{k^2 a_0^2}{\kappa^2} - \frac{2\pi G|k|\sigma_0}{\kappa^2} \tag{6.99}$$

or

$$\frac{\omega^2}{\kappa^2} = 1 + \frac{Q^2}{4}\frac{k^2}{k_T^2} - \frac{|k|}{k_T} \tag{6.100}$$

where Q is the disc stability parameter, defined as :

$$Q = \frac{2k_T a_0}{\kappa} = \frac{\kappa a_0}{\pi G \sigma_0} \tag{6.101}$$

k_T is the *Toomre wave number* defined as :

$$k_T = \frac{\kappa^2}{2\pi G \sigma_0} \tag{6.102}$$

From this expression, the division between stable and unstable solutions occurs when $\omega^2 = 0$ or :

$$\frac{|k|}{k_T} = \frac{2}{Q^2}\left(1 \pm (1 + Q^2)^{1/2}\right) \tag{6.103}$$

This only has a solution for $|k|$ when $Q < 1$. In this case there are regions where $\omega < 0$, hence spiral perturbations grow exponentially, yielding the collapse of clouds, likely resulting into star formation. When $Q > 1 \rightarrow \omega^2 > 0 \forall |k|$ and the disc is always stable. The latter condition can be expressed in terms of a minimum velocity dispersion that makes the disk stable:

$$a_0 \geq a_{0,min} = \frac{\pi G \sigma_0}{\kappa} \tag{6.104}$$

6.6.5 Lindblad Resonances

Returning to the full dispersion relation (eq.6.96) we can write :

$$k^2 a_0^2 - \frac{|k|}{k_T}\kappa^2 + (\kappa^2 - n^2(\Omega_p - \Omega)^2) = 0 \tag{6.105}$$

This is just a quadratic in $|k|$ and, assuming the case $a_0 = a_{0,min}$ it is easy to find that to have real wave-like solutions (i.e. $|k|$ real and positive) it is necessary that :

$$1 \pm \frac{n}{\kappa}(\Omega_p - \Omega) \geq 0 \tag{6.106}$$

and hence :

$$\Omega - \frac{\kappa}{n} \leq \Omega_p \leq \Omega + \frac{\kappa}{n} \tag{6.107}$$

We only have spiral density wave solutions between the inner and outer Lindblad resonances :

- $\Omega_p = \Omega - \frac{\kappa}{n}$ inner Lindblad resonance
- $\Omega_p = \Omega + \frac{\kappa}{n}$ outer Lindblad resonance
- $\Omega_p = \Omega$ is called corotation

6.6.6 The threshold of the Schmidt-Kennicutt relation

The Schmidt-Kennicutt law (relation between the star formation rate surface density and the gas surface density) is know to have a threshold for star formation : below a minimum gas surface density, star formation becomes very inefficient ($\Sigma_{thr}(gas) \sim 5 M_\odot \mathrm{kpc}^{-2}$, but variable from galaxy to galaxy). This is illustrated in Figure 6.16. This threshold is generally responsible for the fact that, despite the gas distribution (HI) extending to large radii, star formation is confined within a certain radius.
The Toomre stability parameter gives a simple explanation for this effect. Indeed, in order to have a instability, i.e. star formation, it has to be $Q < 1$. Therefore,

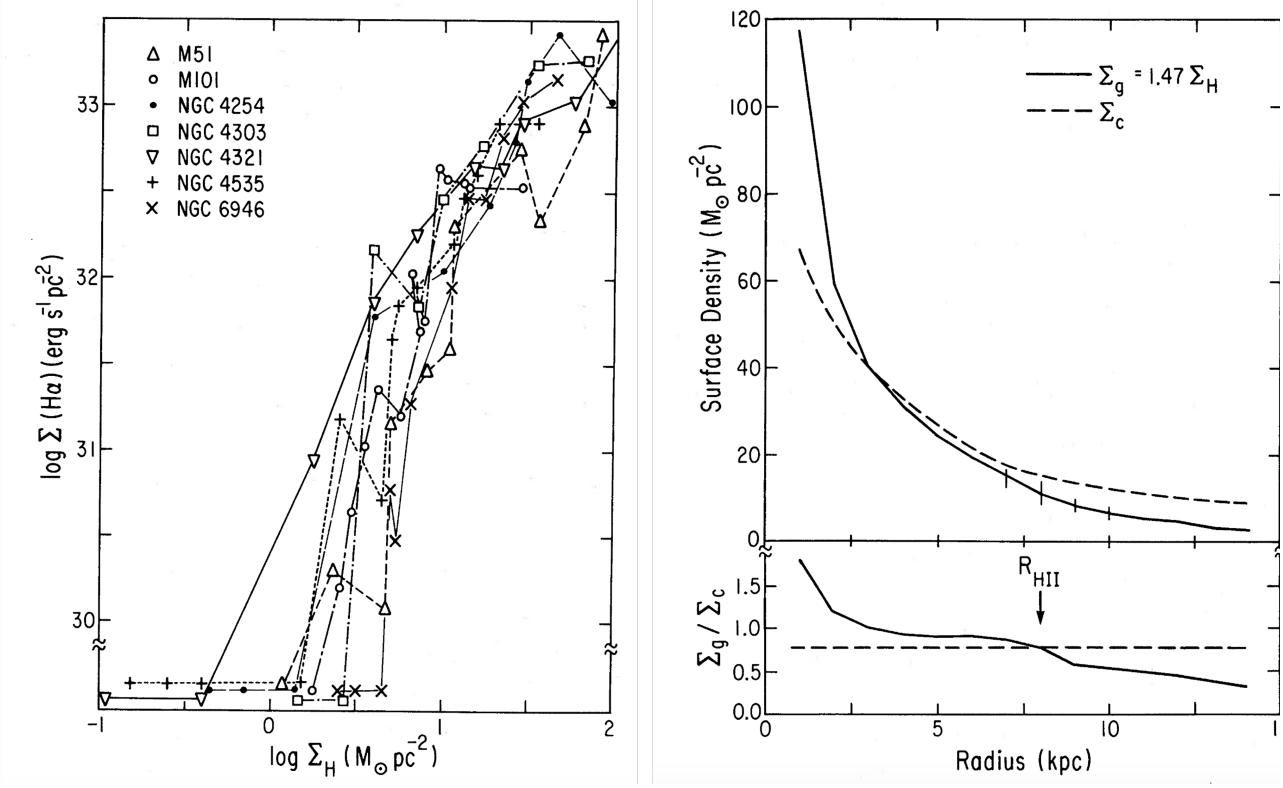

Figure 6.16 : (Left) Dependence of Hα surface luminosity on the total gas surface density - there is clear evidence for a threshold in the Hα emission which is a tracer of the star formation. (Right) Distribution of gas and critical surface density as a function of the radius. The bottom panel shows the ratio of these two quantities and the arrow indicates the edge of the region in which HII regions are found; There are no HII regions, and hence no indication for star-formation, beyond the radius where the gas density falls below a value very close to the critical value. From Kennicutt et al. (1989)

to have star formation the gas surface density has to exceed a critical value :

$$\sigma > \sigma_c = \frac{\kappa a_0}{\pi G} \tag{6.108}$$

It is observed that this condition is indeed met in the central part of disk galaxies, where star formation occurs.